HHS Public Access

Author manuscript

Brain Behav Immun. Author manuscript; available in PMC 2017 March 01.

Published in final edited form as:

Brain Behav Immun. 2016 March ; 53: 84–95. doi:10.1016/j.bbi.2015.11.005.

Intracranial delivery of Interleukin-17A via adeno-associated virus fails to induce physical and learning disabilities and neuroinflammation in mice but improves glucose metabolism through AKT signaling pathway

Junling Yang[a], **Jinghong Kou**[a], **Jeong-Eun Lim**[a], **Robert Lalonde**[b], and **Ken-ichiro Fukuchi**[a,*]

[a]Department of Cancer Biology and Pharmacology, University of Illinois College of Medicine at Peoria, Peoria, Illinois, USA.

[b]Department of Psychology, University of Rouen, Rouen, France.

Abstract

Interleukin-17A (IL-17A) is generally considered as one of the pathogenic factors involved in multiple sclerosis (MS). Indirect evidence for this is that IL-17A-producing T helper 17 (Th17) cells preferentially accumulate in lesions of MS and experimental autoimmune encephalomyelitis (EAE). However, a direct involvement of IL-17A in MS pathogenesis is still an open question. In this study, we overexpressed IL-17A in the brains of mice (IL-17A-in-Brain mice) via recombinant adeno-associated virus serotype 5 (rAAV5)-mediated gene delivery. In spite of high levels of IL-17A expression in the brain and blood, IL-17A-in-Brain mice exhibit no inflammatory responses and no abnormalities in motor coordination and spatial orientation. Unexpectedly, IL-17A-in-Brain mice show decreases in body weight and adipose tissue mass and an improvement in glucose tolerance and insulin sensitivity. IL-17A enhances glucose uptake in PC12 cells by activation of AKT. Our results provide direct evidence for the first time that IL-17A overexpression in the central nervous system does not cause physical and learning disabilities and neuroinflammation and suggest that IL-17A may regulate glucose metabolism through the AKT signaling pathway.

Keywords

IL-17A; multiple sclerosis; experimental autoimmune encephalomyelitis; neuroinflammation; motor coordination; motor activity; glucose tolerance; insulin sensitivity; adipose tissues; AKT

*Corresponding author: Ken-ichiro Fukuchi, MD, PhD, Department of Cancer Biology and Pharmacology, University of Illinois College of Medicine at Peoria, P.O. Box 1649, Peoria, Illinois USA; Phone: 309-671-8545; kfukuchi@uic.edu.

Conflict of interest

The authors declare no conflict of interest.

1. Introduction

Multiple sclerosis (MS) is an autoimmune demyelinating disease of the central nervous system (CNS) causing severe physical and cognitive problems (Rocca et al., 2015; Sumowski and Leavitt, 2013). The mounting evidence suggests that T helper 1 (Th1) and T helper 17 (Th17) cells are the main immunological players, resulting in experimental autoimmune encephalomyelitis (EAE) and MS (Babaloo et al., 2015; Hofstetter et al., 2009; Legroux and Arbour, 2015; Liu et al., 2014; Platten et al., 2009; Tzartos et al., 2008; Wang et al., 2009). Th1 cells, however, migrate across the blood-brain barrier into the CNS less efficiently than Th17 cells (Kebir et al., 2007; Marwaha et al., 2012). Emerging studies show predominant accumulation of Th17 cells in EAE and MS lesions, indirectly indicating that Th17 cells are a key regulator of MS and EAE pathogenesis. Th17 cells produce IL-17A, IL-17F, IL-21 and IL-22 (Kreymborg et al., 2007; Murugaiyan et al., 2015; Nurieva et al., 2007). Among them, IL-17A, signature cytokine of Th17 cells, is often increased in patients with the autoimmune disease (Hemdan et al., 2010; Lock et al., 2002; Matusevicius et al., 1999; Zepp et al., 2011).

IL-17A, cloned in 1993 by Rouvier et al. (Rouvier et al., 1993), is one of the IL-17 family members which also include IL-17B, IL-17C, IL-17D, IL-17E and IL-17F. Among the IL-17 family, IL-17A is most investigated in many inflammatory conditions such as autoimmune diseases (Koenders et al., 2005; Kuchroo et al., 2012; Lubberts et al., 2005) and metabolic disorders (Ahmed and Gaffen, 2010; Ahmed and Gaffen, 2013; Zuniga et al., 2010). It is widely accepted that IL-17A promotes autoimmunity, especially in the context of rheumatoid arthritis (RA), psoriasis, MS and a rodent model of MS, EAE (Kang et al., 2010; Kang et al., 2013; Kulcsar et al., 2014; Lock et al., 2002; Lubberts, 2008; Qian et al., 2007). Indeed, anti-IL-17RA antibodies in clinical trials have shown efficacy in psoriasis, RA and MS (Hueber et al., 2010; Luchtman et al., 2014; Mease et al., 2014; Yang et al., 2014). Furthermore, certain investigators have shown that EAE is substantially reduced in IL-17a$^{-/-}$ or IL-17ar$^{-/-}$ mice (Harrington et al., 2005; Hu et al., 2010; Komiyama et al., 2006). On the contrary, other authors have reported that IL-17a$^{-/-}$ mice are fully susceptible to EAE. There is the possibility that another IL-17 family member, especially IL-17F, which shares about 50% amino-acid sequence identity, may compensate for the loss of IL-17A in IL-17a$^{-/-}$ mice. However, IL-17f$^{-/-}$ mice treated with anti-IL-17A monoclonal antibodies (mAbs) are also fully susceptible to EAE (Haak et al., 2009). In addition, blocking IL-17A alone may not be sufficient for the long-term treatment of MS (Luchtman et al., 2014), indicating that IL-17A itself may not mount a robust inflammatory response in MS pathogenesis (Zenobia and Hajishengallis, 2015). Until now the role of IL-17A in the pathogenesis of MS still remains to be elucidated (Qu et al., 2013; Waisman et al., 2015; Zorzella-Pezavento et al., 2013). To the best of our knowledge, administration or overexpression of IL-17A in the CNS of experimental animals has not been investigated, which could certainly shed some light on the role of IL-17A in MS pathogenesis.

In the present study, we explored the possible effects of IL-17A overexpression in the brain on mouse behavior and pathophysiology via recombinant adeno-associated virus (rAAV)-mediated gene delivery. Our results show that IL-17A overexpression in brain cells neither impaired motor coordination and spatial learning nor cause neuroinflammation. However,

IL-17A overexpression significantly decreased body weight and improved the glucose tolerance in normal chow diet fed adult mice. Furthermore, our cell culture study suggests that IL-17A may increase glucose uptake by neuronal cells through the AKT signaling pathway.

2. Materials and methods

2.1. Recombinant adeno-associated virus preparation

Expression plasmid vector, pAAV-CA, for rAAV production was previously described (Fukuchi et al., 2006). pAAV-CA-IL17A was constructed by cloning mouse IL-17A cDNA under the control of cytomegalovirus enhancer/β-actin promoter in pAAV-CA. The Kozak sequence and woodchuck hepatitis virus post-transcriptional regulatory element were included to increase the transcription and translation efficiency, respectively. Flag sequence encoding DYKDDDDK was placed at the C-terminal ends of IL-17A cDNA as a marker to distinguish it from endogenous IL-17A. The production of rAAV in capsid serotype 5 was performed as previously described (Kou et al., 2011; Kou et al., 2015). The titers of rAAVs were determined as described previously (Fukuchi et al., 2006).

2.2. Experimental animals and intracranial injection of rAAV-IL-17A

For intracranial injection, two-month-old C57BL/6J mice were anesthetized by Nembutal and placed on a stereotaxic instrument with a motorized stereotaxic injector (Stoelting, Wood Dale, IL). A midline incision was made to expose the bregma. A hole in the skull was made by a drill 0.5 mm posterior to the bregma and 1.0 mm right to the midline. rAAV5-IL-17A (1.5×10^{10} vector genomes (vg) in 10 μl PBS/mouse) was injected unilaterally into the right lateral brain ventricle at the depth of 2 mm at a rate of 1 μl/min. Mice subjected to rAAV5-IL-17A injection are referred to as IL-17A-in-Brain mice. Mice similarly treated with 10 μl PBS served as controls and are referred to as PBS-in-Brain mice. All animal protocols were prospectively approved by the Institutional Animal Care and Use Committee of the University of Illinois College of Medicine at Peoria.

2.3. Immunohistochemical analyses

The brains were fixed in 4% paraformaldehyde for 48 h, stored overnight in 30% sucrose in 0.1 M PBS and frozen in Tissue-Tek optimal cutting temperature compound. Coronal sections (35 μm) of the brains were immnuostained with anti-Flag M2 antibody (Sigma, St. Louis, MO), anti-Iba1 antibody (Wako, Osaka, Japan) and anti-GFAP antibody (Serotec, Oxford, UK) for detection of IL-17A, activated microglia and reactive astrocytes, respectively. Endogenous peroxidase was eliminated by 1% H_2O_2 in 10% methanol Tris-buffered saline (TBS) treatment. After washing with 0.1 M Tris buffer (pH 7.5) and 0.1M TBS (pH 7.4), sections were blocked with 5% normal serum in 0.1 M TBS with 0.5% triton-X-100 (TBS-T) and then incubated with primary antibodies in 2% serum in TBS-T for 18–48 h at 4°C. For the negative controls, slides were processed without primary antibody. After rinsing, the sections were incubated with biotinylated secondary antibodies in 2% serum TBS-T for 2 h at room temperature. The avidin-biotin peroxidase method using 3, 3'-diaminobenzidine as a substrate (Vector, Burlingame, CA) was performed. Sections were counterstained with hematoxylin.

2.4 Quantification of M1 and M2 marker and cytokine expression in plasma and brain

Approximately 100 μl blood/mouse was drawn from the tail vein by using microhematocrit heparin tubes (Fisher Scientific, Pittsburgh, PA) and centrifuged for 20 min at 2,000 × g for plasma isolation. Brains were removed under Nembutal anesthesia and the left hemispheres were used for RNA analysis. The right hemispheres were homogenized using the Bio-Plex cell lysis kit (Bio-Rad Laboratories, Hercules, CA) and centrifuged at 12,000 × g for 10 min at 4°C. The supernatants were collected and their protein concentrations were determined by Bio-Rad Protein Assay (Bio-Rad Laboratories, Hercules, CA). Levels of IL-17A, IL-1β, IL-6 and tumor necrosis factor-α (TNF-α) in plasma and brains were determined by ELISA (eBioscience, Inc. San Diego, CA) and/or by western blot analysis. For blood chemistry tests, plasma samples were analyzed by IDEXX BioResearch (West Sacramento, CA). Total RNA from the left hemispheres was isolated using the Direct-zolTM RNA kit (Zymo Research Corporation, Irvine, CA). One to two micrograms of total RNA from each sample were reverse transcribed using oligo (dT)15 primer and SuperScript® III Reverse Transcriptase kit (Life Technologies, Grand Island, NY) to synthesize cDNA. Primer pairs used for real-time PCR are shown in Table 1. The data were analyzed using the comparative Ct method ($2^{-\Delta\Delta CT}$) with β-actin as the normalizer.

2.5. Behavioral schedule and statistics

A battery of behavioral tests was performed on experimental mice at 10 months of age as previously described (Lim et al., 2012). After measuring body weight and adapting mice to handling, the tests were conducted over a 17-day period as follows: spontaneous alternation (days 1–10), open-field (days 1–3), elevated plus-maze (days 4 and 5), stationary beam (day 6), coat-hanger (day 7), rotorod (days 8–10), and Morris water maze (days 11–16). In each test, whenever possible, the apparatus was wiped clean with a wet cloth and dried before the next mouse was introduced to minimize odor cues. Intergroup differences were assessed by a repeated measures analysis of variance (ANOVA) and two-tailed Student's t-test for normally distributed data. In the spontaneous alternation test and the probe trial of the Morris water maze, groups were compared by the Mann-Whitney U test. Whenever possible, results are expressed as mean ± standard error of the mean (SEM). In all cases, $P < 0.05$ was considered to be significant.

2.6. Exploration and anxiety

Spontaneous alternation was measured in a T-maze, made of white acrylic and consisting of a central stem flanked on each side by 2 arms. The maze width was 9 cm, the wall height 20 cm, and each arm 30 cm in length. On the initial trial, the mice were placed in the stem with the right arm blocked by a plastic barrier (forced choice). After entering the available arm, the mice were kept in it for 1 min by closing the barrier behind them. The mice were then retrieved and after removing the barrier, placed back in the stem for a free-choice trial, either into the same arm or the opposite arm (4-paw criterion). On the following 10 days, the same 2-trial procedure was repeated, except that the blocked arm was switched from right on odd days to left on even days. The number of alternations and the latencies before responding during the choice trial were measured. In the absence of any decision within 1 min, the mice

were briefly prodded from behind far from the choice point, usually not more than once, so that a response could be recorded on every trial.

Motor activity was measured in the open-field made of white acrylic with a 50 cm × 50 cm surface area. Each mouse was placed in a corner of the open-field. The activity in central (25 cm × 25 cm surface area) and peripheral zones was recorded in a 5-min session for 3 consecutive days and analyzed by video tracking software (SD Instruments, San Diego, CA). The distance traveled and the time spent resting (<2 cm/s), moving slow (2–5 cm/s), or moving fast (>5 cm/s) in each zone were measured, as well as the time spent in the periphery and center of the apparatus.

The elevated plus-maze consisted of 4 arms in a cross-shaped form 70 cm in length with a 10 cm × 10 cm central region. Two of the arms were enclosed on 3 sides by walls (10 cm in height) facing each other, while the other two were open, except for a minimal border (0.5 cm in height) used to minimize falls. A mouse was placed in the central region and then the number of entries and the time spent inside enclosed and open arms were measured in a 5-min session on 2 consecutive days with the same video tracking system. The open/total arm entries and duration ratios were also calculated.

2.7. Motor coordination

The stationary beam (diameter: 2.5 cm; length: 110 cm) was made of plastic covered by white masking tape to facilitate a firm grip. The beam was divided into 11 segments along its length and placed at a 40-cm height above a cushioned floor to prevent injury. A cardboard wall was inserted at each end to prevent the mouse from escaping. A trial began by placing the mice on the middle segment. The number of segments crossed (4-paw criterion), the latencies before falling, and the number of falls were measured in a single 4-trial session, with a 1 min cut-off period and a 15-min intertrial interval.

Motor speed was measured in the coat-hanger test. The triangular-shaped coat-hanger consisted of a horizontal steel wire (diameter: 2 mm, length: 41 cm) flanked at each end by 2 side-bars (length: 19 cm; inclination: 35° from the horizontal axis). The horizontal bar was placed at a height of 40 cm above a cushioned table. The mice were placed upside-down in the middle of the horizontal wire and released only after gripping with all 4 paws. Seven types of movement time (MT) were compiled, namely latencies before reaching (snout criterion) the first 10 cm segment (MT-1) or the extremity (MT-2) of the horizontal wire, latencies before reaching either side-bar with 2, 3 or 4 paws, and latencies before reaching (snout criterion) either the midway point or the top of the side-bar. Latencies before falling and the number of falls were also compiled. A trial ended whenever the mice either fell or reached the top of the apparatus. In the latter case, a maximal score of 60 s was given for latencies before falling. This test was performed in a single 4-trial session with a 1 min cut-off period and a 15-min intertrial interval.

The accelerating rotorod (Model 7650, Stoelting, Wood Dale, IL) consisted of a beam (diameter: 3 cm) made of ribbed plastic, elevated at a height of 13.5 cm, and separated into 5 sections (width: 5.5 cm) by a plastic barrier. Facing away from the experimenter’s view, the mice were placed on top of the already revolving rod (4 rpm) in the orientation opposite to

its movement, so that falls could be avoided by forward locomotion. The rotorod accelerated gradually and smoothly from 4 to 40 rpm during the 5-min trial. Latencies before falling were measured in 4-trial sessions for 3 days, with a 15-min intertrial interval. Whenever a mouse clung to the rod without moving (passive rotation) for 2 complete revolutions in succession, it was retrieved and a fall registered.

2.8. Spatial learning and memory

The Morris water maze consisted of a pool of blue opaque plastic, 116 cm in diameter with 75-cm high walls, filled with water (20°C) at a height of 31 cm. Powdered milk was evenly spread over the water surface to camouflage the escape platform (8 × 8 cm) made of white plastic and covered with a wire mesh grid to ensure a firm grip. The watered milk was removed every day after a few hours of training and the pool rinsed with clean water. The pool was contained in a room with external visual cues such as light fixtures and a ladder. The mice were placed next to and facing the wall successively in north (N), east (E), south (S), and west (W) positions, with the escape platform hidden 1 cm below water level in the middle of the NW quadrant. The same video tracking equipment was used to estimate path length and escape latencies in 4-trial sessions for 5 days with a 15-min intertrial interval. The mice remained on the platform for at least 5 s. Whenever the mice failed to reach the escape platform within the 1 min cut-off period, they were retrieved from the pool and placed on the platform for 5 s. After swimming, the mice were kept dry in a plastic holding cage filled with paper towels. In the morning after the acquisition phase, a probe trial was conducted by removing the platform and placing the mouse next to and facing the N side. The time spent in the previously correct quadrant was measured for a single 1-min trial. In the afternoon, the visible platform subtask was conducted, with the escape platform lifted 1 cm above water level and shifted to the SE quadrant. A 17-cm high pole was inserted on top of the escape platform as a viewing aid. The same procedure was adopted as with place learning except that the subtest was conducted on a single day.

2.9. Fluorescence-activated cell sorting (FACS)

Nine months after rAAV injection, adipocytes were prepared as previously described (Planat-Benard et al., 2004). In brief, adipose tissues were digested at 37°C in PBS (without calcium and magnesium) containing 2% bovine serum albumin (BSA) and 2 mg/ml collagenase VI (Sigma, St. Louis, MO) for 45 min. After undigested fragments were removed using 100 μm filters (Fisher Scientific, Pittsburgh, PA), adipocytes were separated from pellets of stromal vascular fraction cells by centrifugation at 600g for 10 min. F4/80-PE (eBioscience, Inc. San Diego, CA) and CD206-FITC antibodies (BioLegend, San Diego, CA) were used to identify macrophages and a M2 marker, respectively. Labelled cells were loaded and analyzed by FACS (BD Bioscience, San Jose, CA).

2.10. Intraperitoneal glucose tolerance test (IPGTT) and insulin tolerance test (ITT)

Twenty and thirty weeks after rAAV injection, IPGTT and ITT were conducted, respectively, as previously described (Ize-Ludlow et al., 2011). Animals were fasted for 16 h, weighed and intraperitoneally injected with D-glucose (1.5g/kg) for IPGTT. Blood was obtained using the tail nick method before and at 30, 60, 90 and 120 min after the D-glucose injection for monitoring glucose levels using Glucometer (ReliOn® Prime, Arkray USA,

Minneapolis MN). Plasma insulin levels were determined by insulin ELISA assay kit (Crystal Chem Inc., Downers Grove, IL). For ITT, mice were fasted for 4 h, weighed, and intraperitoneally injected with human insulin (0.75 units/kg, Novolin® R, Novo Nordisk, Princeton, NJ). Blood sugar was monitored before and at 15, 30, 60, and 90 min.

2.11. Cell Culture and western blot analysis

PC12 cells (ATCC® CRL-1721™) were grown in RPMI-1640 medium containing 10% heat-inactivated horse serum (ATCC, Manassas, VA) and 5% heat-inactivated fetal bovine serum (Atlanta Biologicals, Flowery Branch, GA) in humidified 37°C incubator with a 5% CO2 atmosphere. Cells were plated on culture dishes coated with rat tail collagen I (Sigma, St. Louis, MO) at 5×10^5/ml cells. Forty-eight hours after seeding, PC12 cells were treated with 1, 10, 100ng/ml IL-17A (Cell Signaling Technology, Danvers, MA) for 5, 15 and 30 min. The cell lysates were prepared by using radioimmune precipitation assay (RIPA) lysis buffer containing complete miniprotease-inhibitor and phosphatase inhibitor cocktail tablets (Roche Diagnostics Corporation, Indianapolis, IN) and centrifuged at 12,000 × g for 10 min 4°C for collecting supernatants. After determining protein concentrations, the proteins were electrophoresed under reducing conditions in 10% SDS-PAGE gels and transferred to PVDF membranes. The membranes were incubated overnight at 4°C with anti-phospho-AKT and anti-AKT antibody (1:1000 dilution) (Cell Signaling Technology, Danvers, MA) and specific bands were visualized by an enhanced chemiluminescence system (Amersham, Arlington Heights, IL). The optical densities of the protein bands were determined by densitometric scanning using an HP Scanjet G3010 Photo Scanner and Image J V1.40 (NIH, MD). The optical density of p-AKT band was divided by that of total AKT band on the same lane from the same membrane for normalization.

2.12. Glucose uptake

The fluorescent glucose analog, 2-deox-2-[(7-nitro-2,1,3-benzoxadiazol-4-yl)amino]-D-glucose (2-NBDG) uptake assay was performed by the manufacturer's protocol (Cayman Chemical, Ann Arbor, MI). PC12 cells were seeded in 35mm dishes at a density of 5×10^5 cells/ml in serum-free medium overnight. The next day, the medium was replaced with fresh glucose-free, serum-free medium. Cells were pretreated with or without 25 μM AKT1/2 inhibitor, A6730 (Sigma, St. Louis, MO), for 30 min followed by treatment with or without 100ng/ml of IL-17A or nerve growth factor (NGF) (Biomedical Technologies, Ward Hill, MA) for another 30 min. Then, 2-NBDG was added to the medium. Ten minutes later, cells were harvested, washed and analyzed by FACS.

2.13. Statistical analysis

Data were expressed as mean ± SEM. The data were analyzed using SPSS version 22 software (IBM, Armonk, NY). An independent sample t test was used for statistical comparisons between the two groups. One-way ANOVA followed by a least-significant-difference test was used for statistical comparisons among multiple groups. P values less than 0.05 were considered statistically significant.

3. Results

3.1. Overexpression of IL-17A in mouse brain via rAAV5-mediated gene delivery does not cause inflammatory responses

The Flag tag was added to the C-terminal end of IL-17A in order to distinguish endogenous IL-17A from IL-17A produced from the rAAV-IL-17A vector. The Flag tag may hamper biological function of IL-17A. Therefore, we tested biological activity of IL-17A produced by the AAV-IL-17A vector using 3T3 cells (NIH/Swiss mouse fibroblast). IL-17A induces the production and secretion of interleukin-6 (IL-6) in 3T3 cells in a dose-dependent manner and this feature of 3T3 cells has been used to quantify biological activity of synthetic or recombinant IL-17A (Ruddy et al., 2004). First, rAAV1-IL-17A was injected into the thigh muscles of C57BL/6 mice and a high level of IL-17A (32 ng/ml) in the plasma isolated from one of the mice was confirmed by IL-17A ELISA (Supplementary data). Treatment of 3T3 cells with the plasma significantly increased IL-6 production and the increase in IL-6 was abolished by neutralizing the plasma with anti-IL-17A antibody, indicating that plasma IL-17A derived from the rAAV-IL-17 vector is biologically functional (Supplementary Fig. S1).

To determine the potential role of IL-17A in the CNS, we established IL-17A-in-Brain mice by injecting rAAV5-IL-17A into the cerebral ventricles of C57BL/6 mice. Three months after injection, IL-17A was identified as a 16 kDa fragment in the brain by western blotting using anti-Flag antibody (Fig. 1A). Five months after injection, IL-17A in the brain was visualized by immunohistochemistry (Fig. 1B and C). IL-17A expression was found throughout the hippocampi and partly in the neocortex. Nine months after injection, the average plasma IL-17A level in IL-17A-in-Brain mice was 6.22 ± 0.48 ng/ml while plasma IL-17A was undetectable by ELISA in PBS-in-Brain mice (Fig. 1D). Thus, IL-17A appeared to be secreted from brain cells and reached the peripheral circulation.

IL-17A overexpression may induce microglial activation, leukocyte infiltration and cytokine production in the brain. Therefore, the brain sections were subjected to histochemistry by hematoxylin and eosin (H & E) staining for mononuclear cell infiltration and immunohistochemistry by anti-Iba1 and anti-GFAP antibodies for detection of activated microglia and reactive astrocytes, respectively. Infiltrating mononuclear cells were not found in the brains of the experimental mice and no difference was found in Iba1 and GFAP immunostaining between IL-17A-in-Brain and PBS-in-Brain mice (data not shown). We further determined expression levels of M1 and M2 microglia/macrophage markers and cytokines in the brain by quantitative PCR, which included interferon-γ (IFN-γ), IL-1β, IL-6, TNF-α, arginase 1 (Arg1), chitinase 3-like 3 (also known as YM1) and transforming growth factor-β. There were no differences in the expression levels of these markers and cytokines between IL-17A-in-Brain and PBS-in-Brain mice 9 months after injection (Fig. 2A). In addition, blood chemistry tests were performed to assess the function of major organs and included triglyceride, total cholesterol, blood urea nitrogen, creatinine, total protein, globulin, albumin, creatine phosphokinase, aspartate aminotransferase, alanine transaminase and growth hormone. All values of these blood test results were within normal ranges and showed no significant differences between the two groups (Fig. 2B;

Supplementary Fig. S2). There was neither clear indication of increases in IL-1β, IL-6 and TNF-α in pooled plasma from IL-17A-in-Brain and PBS-in-Brain mice nor significant differences in food consumption and body temperature between IL-17A-in-Brain and PBS-in-Brain mice (data not shown). These results indicate that overexpression of IL-17A in the brain does not induce inflammatory responses.

3.2. Overexpression of IL-17A does not impair motor coordination and spatial learning and memory

Overexpression of IL-17A may induce autoimmune disease such as MS and RA. Therefore, we carried out a battery of behavior tests to examine possible behavioral changes in animals 8 months after rAAV or PBS injection.

3.2.1. Exploration and anxiety—In the T-maze spontaneous alteration test, PBS-in-brain mice alternated above chance (P=0.005) while IL-17A-in-Brain mice did not (P=0.233) (Fig. 3A). The latencies of alteration did not show any difference (P=0.576) (Fig. 3B). In the open-field, IL-17A-in-Brain mice were more active in the central part of the open-field (28.38 ± 2.28%) than PBS-in-Brain mice (18.50 ± 3.10%) on day 1 of testing (P=0.024). In contrast, this effect was not found in the peripheral part of the open-field, nor was there any effect on the following day (Fig. 4). No intergroup difference emerged in the plus-maze test (Table 2).

3.2.2. Motor coordination—In the stationary beam test (Fig. 5A), there was no difference in segments crossed in IL-17A-Brain mice or latencies before falling (240 ± 0.00 s for PBS-in-Brain vs. 237 ±3.33 s for IL-17A-Brain, P= 0.281). In the coat-hanger test (Fig. 5B), the latency of MT-2 was shorter in the IL-17A-in-Brain group than that in the PBS-in-Brain group (P=0.022). There were no differences in any other latencies between the two groups. On the rotorod (Fig. 5C), the mice performed better on day 3 compared to day 1 in both groups but no intergroup differences were found.

3.2.3. Spatial learning and memory—In the acquisition phase of the Morris water maze, there were significant reductions in latencies and path lengths between days (P=0.0005) (Fig. 6A, B). There was no difference between the two groups in either latencies or path lengths (Fig 6A. B). In the probe trial, the percentages of time spent in the correct quad were 26.55 ± 0.96% for IL-17A-in-Brain mice and 26.71 ± 1.31% for PBS-in-Brain mice (P=0.92) (Fig. 6C). In the visible platform subtask, the latencies and distance travelled were 29.87 ± 3.67 s and 456.07 ± 65.01 cm in IL-17A-in-Brain mice and 34.37 ± 7.24 s and 463.55 ± 71.01 cm in PBS-in-Brain mice (P > 0.05). Thus, no differences were found in any measure between the two groups.

3.3 Overexpression of IL-17A reduces body weight and improves glucose metabolism

The first significant difference in body weight between IL-17A-in-Brain and PBS-in-Brain mice was discernible 4 weeks after injection (P < 0.05) and, thereafter, the degree of difference (P < 0.01) increased between the two groups (Fig. 7A). Nine month after the injection, the average weight of right epididymal adipose tissues in IL-17A-in-Brain mice (0.329 ± 0.056 g) was approximately one third of that in PBS-in-Brain mice (0.909 ± 0.066

g; $P < 0.001$) (Fig. 7B). H&E stained adipose tissue sections revealed that the size of adipocytes is smaller in IL-17A-in-Brain than in PBS-in-Brain mice (Fig. 7C). M2 macrophages in epididymal adipose tissue were analyzed by FACS. The percentages of $CD206^+$ $F4/80^+$ M2 macrophages in $F4/80^+$ cells in IL-17A-Brain (88.21 ± 7.06%) were higher than those in PBS-in-Brain mice (84.96 ± 2.86%; $P < 0.05$) (Fig. 7D). Thus, overexpression of IL-17A reduced adipocyte mass and increased percentage of M2 macrophages in epididymal adipose tissues.

Blood glucose and insulin levels in IL-17A-in-Brain mice were significantly lower than those in PBS-in-Brain mice throughout IPGTT (Fig. 7E and F; $P < 0.01$). Consistent with these results, IL-17A-in-Brain mice showed increased insulin sensitivity in ITT (Fig. 7G; $P < 0.05$).

3.4. IL-17A enhances glucose uptake in PC12 cells by activation of AKT

PC12 cell is a pheochromocytoma cell line derived from the rat adrenal medulla and widely used to induce neuronal differentiation by NGF. In order to explore the possible mechanism of IL-17A in glucose metabolism in neurons, PC12 cell were treated with IL-17A (1, 10, and 100ng/ml). Phospho-AKT in PC12 cells increased in a dose-and time-dependent manner (Fig. 8A and B). After incubating with IL-17A or NGF (100ng/ml) for 30 min, the percentage of glucose uptake by PC12 cells was significantly increased to 42.97 ± 2.45% or 42.50 ± 2.83%, respectively, compared to 36.07 ± 2.05% in control ($P < 0.05$) (Fig. 8C and D). A6730 (AKT1/2 kinase inhibitor) significantly inhibited the increased glucose uptake by IL-17A (30.05 ± 3.41%; $P < 0.01$) while A6730 alone did not alter glucose uptake (34.21 ± 5.56%) compared with control (Fig. 8 D; $P > 0.05$).

In addition, hippocampal slices were used as an ex vivo model. IL-17A treatment (100 ng/ml) for 15 and 30 min significantly increased phospho-AKT in the hippocampal slices (Supplementary Fig. S3; $P < 0.01$).

4. Discussion

IL-17A is generally considered as a damaging, proinflammatory cytokine involved in many inflammatory diseases, including MS and RA (Ferreira et al., 2014; Fletcher et al., 2010; McFarland and Martin, 2007). Emerging evidence, however, supports the notion that IL-17A may play a protective role in tissue repair and inflammation (Gopal et al., 2014; Littman and Rudensky, 2010; Nascimento et al., 2015; Nishikawa et al., 2014; O'Connor, Jr. et al., 2009). Likewise, studies in MS and EAE led to conflicting results on the role of IL-17A in disease development (Haak et al., 2009; Harrington et al., 2005; Hu et al., 2010; Komiyama et al., 2006; Luchtman et al., 2014; Niimi et al., 2013). Based on a two-wave hypothesis, IL-17A-producing Th17 cells after priming in peripheral lymph nodes traffic through the choroid plexus into the subarachnoid space where Th17 cells are restimulated by macrophages to undergo clonal expansion. IL-17A secreted from Th17 cells in the subarachnoid space activate the parenchymal vasculature followed by accumulation of leukocytes leading to the explosive inflammatory responses associated with the onset of EAE (Kang et al., 2013). IL-17A levels are significantly elevated in MS and EAE (Ishizu et al., 2005; Jiang et al., 2012; Kostic et al., 2014; Lock et al., 2002; Matusevicius et al., 1999).

Moreover, IL-17A neutralization improves and adoptive transfer of myelin-specific Th17 cells exacerbates clinical conditions of EAE mice (Hofstetter et al., 2005; Jager et al., 2009; Mardiguian et al., 2013). However, the targets of IL-17A signals in CNS-resident cells are still not clear (Waisman et al., 2015). Additionally, there is a possibility that other cytokines, other than IL-17A, produced by Th17 cells, may also contribute to onset and development of MS (Graeber and Olsen, 2012). In view of the fact that the role of IL-17A in CNS inflammatory diseases is unsettled, this study is the first to overexpress IL-17A in the mouse CNS to uncover the potential role of IL-17A.

MS patients show a wide variety of neurological symptoms, including paresthesia or numbness, motor weakness, incoordination, gait disturbance, and cognitive impairment (Cree, 2014; Miller and Leary, 2007; Milo and Miller, 2014). As seen in humans, certain behavioral changes can be observed in EAE mice (Acharjee et al., 2013; Franco-Pons et al., 2007; Jones et al., 2008; Legroux and Arbour, 2015; Moore et al., 2014; Serra-de-Oliveira et al., 2015; Ulrich et al., 2010; Wang et al., 2013). Clinical signs and paralysis in EAE mice are scored on a scale from 0 (clinically normal) to 5 (moribund) (Miller et al., 2010). In our study, IL-17A-in-Brain mice did not show any clinical signs and abnormal behaviors and their EAE clinical score remained at 0 throughout the experiments. To discern subtle changes in physical activities and cognitive functions which may be induced by IL-17A overexpression in the brain, we performed a battery of behavioral tests including T-maze, open-field, elevated plus-maze, stationary beam, coat-hanger, accelerating rotorod and Morris water maze. Surprisingly, IL-17A overexpression in the mouse brain did not cause significant alterations in the majority of the measures in these behavioral tests. More surprisingly, there was a significant difference in MS-2 in the coat hanger test, which indicates IL-17A-in-Brain mice move faster to reach the extremity of the horizontal wire in a coat-hanger than PBS-in-Brain mice. In addition, although anxiety disorders commonly occur in patients with MS (Korostil and Feinstein, 2007; Michalski et al., 2010; Theaudin et al., 2015), IL-17A-in-Brain mice did not show increased anxiety in T-maze, open-field and plus-maze compared to PBS-in-Brain mice. Instead, IL-17A-in-Brain mice were more active in the central part of the open-field (day 1 only) than PBS-in-Brain mice. This effect was not found in the peripheral part of the open-field, indicating a decrease in anxiety without hyperactivity. The decrease in anxiety did not generalize to the T-maze and plus maze tests, perhaps because of the higher degree in anxiety involved in exploring open spaces. PBS-in-Brain mice alternated significantly above chance but IL-17-in-Brain mice did not. Because circulating glucose levels are known to influence spontaneous alternation performance in rodents (Ragozzino et al., 1996), poor performance on the T-maze may be explained by low blood glucose in IL-17A-in-Brain mice. Our results from water maze indicate that IL-17A overexpression in the brain does not provoke cognitive decline. Taken together, our behavioral data show that overexpression of IL-17A in the mouse CNS does not induce deficits in physical activities and cognitive functions.

Microglia activation in the CNS is considered to be a crucial step in development of EAE and contributes to dendritic pathology and neuronal loss by releasing cytokines, such as IL-6, and TNF-α (Centonze et al., 2009; Lassmann, 2014; Trebst et al., 2001; Zager et al., 2015). We, however, did not find increases in mRNA and protein levels of brain IL-6 and TNF-α in IL-17A-in-Brain mice. IL-17A overexpression did not increase expression levels

of IBA1, a microglia marker, and GFAP, an astrocyte marker, also. Furthermore, we also did not find differences in brain expression levels of M1 and M2 inflammation markers between IL-17A-in-Brain and PBS-in-Brain mice (Fig. 2). Although plasma IL-17A levels increased in IL-17A-in-Brain mice, other proinflammatory cytokines including IL-1β, IL-6 and TNF-α did not. The blood chemistry profile, which reflects the functions of liver, kidney, muscle, and lipid metabolism, showed no abnormality and no difference between IL-17A-in-Brain and PBS-in-Brain mice. Worth noting, the percentage of anti-inflammatory macrophage (M2), rather than pro-inflammatory macrophage (M1), in adipose tissue of IL-17A-in-Brain mice significantly increased compared with that in PBS-in-Brain mice. Our data support the notion that IL-17A may become a pathogenic cytokine only when it synergizes with other cytokines and immune cells, such as TNF-α (Gu et al., 2013; Liu et al., 2011; Schwandner et al., 2000) and interleukin-1 β (Hirota et al., 2007), which are increased neither in brain nor in plasma in our IL-17A-in-Brain mice (Fig. 2). Alternatively, IL-17A may need to be expressed by peripheral immune cells such as Th17 cells and γδ T cells in order to induce infiltration of immune cells into the CNS (Gelderblom et al., 2012; Kebir et al., 2007).

Recently, increased prevalence of insulin resistance and impaired glucose tolerance in MS patients was reported (Oliveira et al., 2014; Penesova et al., 2015; Wens et al., 2013). In previous studies, IL-17A inhibited adipogenesis and moderated adipose tissue accumulation in vitro and IL-17a$^{-/-}$ mice showed increased bodyweight, glucose tolerance and insulin sensitivity (Ahmed and Gaffen, 2010; Ahmed and Gaffen, 2013; Straus, 2013; Winer et al., 2009; Zuniga et al., 2010). Therefore, altered expression of IL-17A may induce impaired glucose metabolism in MS patients. In the previous studies, however, effects of increased levels of IL-17A on glucose metabolism and obesity in vivo were uninvestigated and remained unknown. In the current study, IL-17A-in-Brain mice showed improved glucose tolerance and insulin resistance, together with the loss of bodyweight and fat pad weight.

The phosphoinositide 3-kinase (PI3K)-AKT signaling pathway is one of the main insulin signaling pathways to regulate glucose uptake (Taniguchi et al., 2006). NGF activates AKT and enhances glucose uptake in PC12 cells by activation of its receptor, TrkA, which interacts with insulin receptor and insulin receptor substrate 1 (Geetha et al., 2013). Interestingly, an increasing body of evidence has shown that NGF and IL-17 share certain structural (cysteine knot fold) (Hymowitz et al., 2001; Zhang et al., 2011) and functional resemblances (Chisholm et al., 2012; Li et al., 2011). Therein, we explored the possible effect of IL-17A on glucose use in PC12 cells. As is the case of NGF, IL-17A enhanced the glucose uptake by activating AKT signaling, which can be inhibited by AKT1/2 inhibitor. Moreover, P-AKT was also increased in ex vivo hippocampus slice cultures by IL-17A. Our findings suggest that IL-17A may increase glucose uptake in vivo via activation of AKT and improve the glucose metabolism.

In conclusion, our present study explored for the first time the potential role of IL-17A in the CNS by creating mice that overexpress IL-17A in the brain. We demonstrate that IL-17A-in-Brain mice do not develop behavioral abnormalities and CNS inflammation but show improved glucose metabolism. Furthermore, our data show that IL-17A may improve

glucose tolerance by activating AKT. Accordingly, careful consideration should be given to ongoing clinical trials when IL-17A inhibitors are used.

Supplementary Material

Refer to Web version on PubMed Central for supplementary material.

Acknowledgments

We thank Dr. David Wasserman, Director, Mouse Metabolic Phenotyping Center and AM Lyle Chair in Diabetes Research (Vanderbilt University Medical Center) for helpful discussions and suggestions and Ms. Linda Walter (University of Illinois College of Medicine at Peoria) for assistance in preparation of this manuscript. This work was supported in part by grants from the National Institutes of Health (AG030399 and AG037814).

References

Acharjee S, Nayani N, Tsutsui M, Hill MN, Ousman SS, Pittman QJ. Altered cognitive-emotional behavior in early experimental autoimmune encephalitis--cytokine and hormonal correlates. Brain Behav Immun. 2013; 33:164–172. [PubMed: 23886782]

Ahmed M, Gaffen SL. IL-17 in obesity and adipogenesis. Cytokine Growth Factor Rev. 2010; 21:449–453. [PubMed: 21084215]

Ahmed M, Gaffen SL. IL-17 inhibits adipogenesis in part via C/EBPalpha, PPARgamma and Kruppel-like factors. Cytokine. 2013; 61:898–905. [PubMed: 23332504]

Babaloo Z, Aliparasti MR, Babaiea F, Almasi S, Baradaran B, Farhoudi M. The role of Th17 cells in patients with relapsing-remitting multiple sclerosis: interleukin-17A and interleukin-17F serum levels. Immunol Lett. 2015; 164:76–80. [PubMed: 25625963]

Centonze D, Muzio L, Rossi S, Cavasinni F, De CV, Bergami A, Musella A, D'Amelio M, Cavallucci V, Martorana A, Bergamaschi A, Cencioni MT, Diamantini A, Butti E, Comi G, Bernardi G, Cecconi F, Battistini L, Furlan R, Martino G. Inflammation triggers synaptic alteration and degeneration in experimental autoimmune encephalomyelitis. J Neurosci. 2009; 29:3442–3452. [PubMed: 19295150]

Chisholm SP, Cervi AL, Nagpal S, Lomax AE. Interleukin-17A increases neurite outgrowth from adult postganglionic sympathetic neurons. J Neurosci. 2012; 32:1146–1155. [PubMed: 22279201]

Cree BA. Acute inflammatory myelopathies. Handb Clin Neurol. 2014; 122:613–667. [PubMed: 24507538]

Ferreira TB, Hygino J, Barros PO, Teixeira B, Kasahara TM, Linhares UC, Lopes LM, Vasconcelos CC, Alvarenga R, Wing AC, Andrade RM, Andrade AF, Bento CA. Endogenous interleukin-6 amplifies interleukin-17 production and corticoid-resistance in peripheral T cells from patients with multiple sclerosis. Immunology. 2014; 143:560–568. [PubMed: 24919524]

Fletcher JM, Lalor SJ, Sweeney CM, Tubridy N, Mills KH. T cells in multiple sclerosis and experimental autoimmune encephalomyelitis. Clin Exp Immunol. 2010; 162:1–11. [PubMed: 20682002]

Franco-Pons N, Torrente M, Colomina MT, Vilella E. Behavioral deficits in the cuprizone-induced murine model of demyelination/remyelination. Toxicol Lett. 2007; 169:205–213. [PubMed: 17317045]

Fukuchi KI, Tahara K, Kim HD, Maxwell JA, Lewis TL, Accavitti-Loper M, Kim H, Ponnazhagan S, Lalonde R. Anti-Aβ single chain antibody delivery *via* adeno-associated virus for treatment of Alzheimer's disease. Neurobiol Dis. 2006; 23:502–511. [PubMed: 16766200]

Geetha T, Rege SD, Mathews SE, Meakin SO, White MF, Babu JR. Nerve growth factor receptor TrkA, a new receptor in insulin signaling pathway in PC12 cells. J Biol Chem. 2013; 288:23807–23813. [PubMed: 23749991]

Gelderblom M, Weymar A, Bernreuther C, Velden J, Arunachalam P, Steinbach K, Orthey E, Arumugam TV, Leypoldt F, Simova O, Thom V, Friese MA, Prinz I, Holscher C, Glatzel M, Korn

T, Gerloff C, Tolosa E, Magnus T. Neutralization of the IL-17 axis diminishes neutrophil invasion and protects from ischemic stroke. Blood. 2012; 120:3793–3802. [PubMed: 22976954]

Gopal R, Monin L, Slight S, Uche U, Blanchard E, Fallert Junecko BA, Ramos-Payan R, Stallings CL, Reinhart TA, Kolls JK, Kaushal D, Nagarajan U, Rangel-Moreno J, Khader SA. Unexpected role for IL-17 in protective immunity against hypervirulent Mycobacterium tuberculosis HN878 infection. PLoS Pathog. 2014; 10:e1004099. [PubMed: 24831696]

Graeber KE, Olsen NJ. Th17 cell cytokine secretion profile in host defense and autoimmunity. Inflamm Res. 2012; 61:87–96. [PubMed: 22197935]

Gu C, Wu L, Li X. IL-17 family: cytokines, receptors and signaling. Cytokine. 2013; 64:477–485. [PubMed: 24011563]

Haak S, Croxford AL, Kreymborg K, Heppner FL, Pouly S, Becher B, Waisman A. IL-17A and IL-17F do not contribute vitally to autoimmune neuro-inflammation in mice. J Clin Invest. 2009; 119:61–69. [PubMed: 19075395]

Harrington LE, Hatton RD, Mangan PR, Turner H, Murphy TL, Murphy KM, Weaver CT. Interleukin 17-producing CD4+ effector T cells develop via a lineage distinct from the T helper type 1 and 2 lineages. Nat Immunol. 2005; 6:1123–1132. [PubMed: 16200070]

Hemdan NY, Birkenmeier G, Wichmann G, Abu El-Saad AM, Krieger T, Conrad K, Sack U. Interleukin-17-producing T helper cells in autoimmunity. Autoimmun Rev. 2010; 9:785–792. [PubMed: 20647062]

Hirota K, Yoshitomi H, Hashimoto M, Maeda S, Teradaira S, Sugimoto N, Yamaguchi T, Nomura T, Ito H, Nakamura T, Sakaguchi N, Sakaguchi S. Preferential recruitment of CCR6-expressing Th17 cells to inflamed joints via CCL20 in rheumatoid arthritis and its animal model. J Exp Med. 2007; 204:2803–2812. [PubMed: 18025126]

Hofstetter H, Gold R, Hartung HP. Th17 cells in MS and experimental autoimmune encephalomyelitis. Int MS J. 2009; 16:12–18. [PubMed: 19413921]

Hofstetter HH, Ibrahim SM, Koczan D, Kruse N, Weishaupt A, Toyka KV, Gold R. Therapeutic efficacy of IL-17 neutralization in murine experimental autoimmune encephalomyelitis. Cell Immunol. 2005; 237:123–130. [PubMed: 16386239]

Hu Y, Ota N, Peng I, Refino CJ, Danilenko DM, Caplazi P, Ouyang W. IL-17RC is required for IL-17A- and IL-17F–dependent signaling and the pathogenesis of experimental autoimmune encephalomyelitis. J Immunol. 2010; 184:4307–4316. [PubMed: 20231694]

Hueber W, Patel DD, Dryja T, Wright AM, Koroleva I, Bruin G, Antoni C, Draelos Z, Gold MH, Durez P, Tak PP, Gomez-Reino JJ, Foster CS, Kim RY, Samson CM, Falk NS, Chu DS, Callanan D, Nguyen QD, Rose K, Haider A, Di PF. Effects of AIN457, a fully human antibody to interleukin-17A, on psoriasis, rheumatoid arthritis, and uveitis. Sci Transl Med. 2010; 2:52ra72.

Hymowitz SG, Filvaroff EH, Yin JP, Lee J, Cai L, Risser P, Maruoka M, Mao W, Foster J, Kelley RF, Pan G, Gurney AL, de Vos AM, Starovasnik MA. IL-17s adopt a cystine knot fold: structure and activity of a novel cytokine, IL-17F, and implications for receptor binding. EMBO J. 2001; 20:5332–5341. [PubMed: 11574464]

Ishizu T, Osoegawa M, Mei FJ, Kikuchi H, Tanaka M, Takakura Y, Minohara M, Murai H, Mihara F, Taniwaki T, Kira J. Intrathecal activation of the IL-17/IL-8 axis in opticospinal multiple sclerosis. Brain. 2005; 128:988–1002. [PubMed: 15743872]

Ize-Ludlow D, Lightfoot YL, Parker M, Xue S, Wasserfall C, Haller MJ, Schatz D, Becker DJ, Atkinson MA, Mathews CE. Progressive erosion of beta-cell function precedes the onset of hyperglycemia in the NOD mouse model of type 1 diabetes. Diabetes. 2011; 60:2086–2091. [PubMed: 21659497]

Jager A, Dardalhon V, Sobel RA, Bettelli E, Kuchroo VK. Th1, Th17, and Th9 effector cells induce experimental autoimmune encephalomyelitis with different pathological phenotypes. J Immunol. 2009; 183:7169–7177. [PubMed: 19890056]

Jiang HR, Milovanovic M, Allan D, Niedbala W, Besnard AG, Fukada SY, Alves-Filho JC, Togbe D, Goodyear CS, Linington C, Xu D, Lukic ML, Liew FY. IL-33 attenuates EAE by suppressing IL-17 and IFN-gamma production and inducing alternatively activated macrophages. Eur J Immunol. 2012; 42:1804–1814. [PubMed: 22585447]

Jones MV, Nguyen TT, Deboy CA, Griffin JW, Whartenby KA, Kerr DA, Calabresi PA. Behavioral and pathological outcomes in MOG 35–55 experimental autoimmune encephalomyelitis. J Neuroimmunol. 2008; 199:83–93. [PubMed: 18582952]

Kang Z, Altuntas CZ, Gulen MF, Liu C, Giltiay N, Qin H, Liu L, Qian W, Ransohoff RM, Bergmann C, Stohlman S, Tuohy VK, Li X. Astrocyte-restricted ablation of interleukin-17-induced Act1-mediated signaling ameliorates autoimmune encephalomyelitis. Immunity. 2010; 32:414–425. [PubMed: 20303295]

Kang Z, Wang C, Zepp J, Wu L, Sun K, Zhao J, Chandrasekharan U, DiCorleto PE, Trapp BD, Ransohoff RM, Li X. Act1 mediates IL-17-induced EAE pathogenesis selectively in NG2+ glial cells. Nat Neurosci. 2013; 16:1401–1408. [PubMed: 23995070]

Kebir H, Kreymborg K, Ifergan I, Dodelet-Devillers A, Cayrol R, Bernard M, Giuliani F, Arbour N, Becher B, Prat A. Human TH17 lymphocytes promote blood-brain barrier disruption and central nervous system inflammation. Nat Med. 2007; 13:1173–1175. [PubMed: 17828272]

Koenders MI, Lubberts E, Oppers-Walgreen B, van den Bersselaar L, Helsen MM, Di Padova FE, Boots AM, Gram H, Joosten LA, van den Berg WB. Blocking of interleukin-17 during reactivation of experimental arthritis prevents joint inflammation and bone erosion by decreasing RANKL and interleukin-1. Am J Pathol. 2005; 167:141–149. [PubMed: 15972960]

Komiyama Y, Nakae S, Matsuki T, Nambu A, Ishigame H, Kakuta S, Sudo K, Iwakura Y. IL-17 plays an important role in the development of experimental autoimmune encephalomyelitis. J Immunol. 2006; 177:566–573. [PubMed: 16785554]

Korostil M, Feinstein A. Anxiety disorders and their clinical correlates in multiple sclerosis patients. Mult Scler. 2007; 13:67–72. [PubMed: 17294613]

Kostic M, Dzopalic T, Zivanovic S, Zivkovic N, Cvetanovic A, Stojanovic I, Vojinovic S, Marjanovic G, Savic V, Colic M. IL-17 and glutamate excitotoxicity in the pathogenesis of multiple sclerosis. Scand J Immunol. 2014; 79:181–186. [PubMed: 24383677]

Kou J, Kim HD, Pattanyak A, Song M, Lim J, Taguchi H, Paul S, Cirrito JR, Ponnazhagan S, Fukuchi K. Anti-Abeta single-chain antibody brain delivery via AAV reduces amyloid load but may increase cerebral hemorrhages in an Alzheimer mouse model. J Alzheimers Dis. 2011; 27:23–28. [PubMed: 21709371]

Kou J, Yang J, Lim JE, Pattanayak A, Song M, Planque S, Paul S, Fukuchi K. Catalytic immunoglobulin gene delivery in a mouse model of Alzheimer's disease: prophylactic and therapeutic applications. Mol Neurobiol. 2015; 51:43–56. [PubMed: 24733587]

Kreymborg K, Etzensperger R, Dumoutier L, Haak S, Rebollo A, Buch T, Heppner FL, Renauld JC, Becher B. IL-22 is expressed by Th17 cells in an IL-23-dependent fashion, but not required for the development of autoimmune encephalomyelitis. J Immunol. 2007; 179:8098–8104. [PubMed: 18056351]

Kuchroo VK, Ohashi PS, Sartor RB, Vinuesa CG. Dysregulation of immune homeostasis in autoimmune diseases. Nat Med. 2012; 18:42–47. [PubMed: 22227671]

Kulcsar KA, Baxter VK, Greene IP, Griffin DE. Interleukin 10 modulation of pathogenic Th17 cells during fatal alphavirus encephalomyelitis. Proc Natl Acad Sci U S A. 2014; 111:16053–16058. [PubMed: 25362048]

Lassmann H. Mechanisms of white matter damage in multiple sclerosis. Glia. 2014; 62:1816–1830. [PubMed: 24470325]

Legroux L, Arbour N. Multiple sclerosis and T lymphocytes: an entangled story. J Neuroimmune Pharmacol. 2015

Li Z, Burns AR, Han L, Rumbaut RE, Smith CW. IL-17 and VEGF are necessary for efficient corneal nerve regeneration. Am J Pathol. 2011; 178:1106–1116. [PubMed: 21356362]

Lim JE, Song M, Jin J, Kou J, Pattanayak A, Lalonde R, Fukuchi K. The effects of MyD88 deficiency on exploratory activity, anxiety, motor coordination, and spatial learning in C57BL/6 and APPswe/PS1dE9 mice. Behav Brain Res. 2012; 227:36–42. [PubMed: 22051943]

Littman DR, Rudensky AY. Th17 and regulatory T cells in mediating and restraining inflammation. Cell. 2010; 140:845–858. [PubMed: 20303875]

Liu X, He F, Pang R, Zhao D, Qiu W, Shan K, Zhang J, Lu Y, Li Y, Wang Y. Interleukin-17 (IL-17)-induced microRNA 873 (miR-873) contributes to the pathogenesis of experimental autoimmune

encephalomyelitis by targeting A20 ubiquitin-editing enzyme. J Biol Chem. 2014; 289:28971–28986. [PubMed: 25183005]

Liu Y, Mei J, Gonzales L, Yang G, Dai N, Wang P, Zhang P, Favara M, Malcolm KC, Guttentag S, Worthen GS. IL-17A and TNF-alpha exert synergistic effects on expression of CXCL5 by alveolar type II cells in vivo and in vitro. J Immunol. 2011; 186:3197–3205. [PubMed: 21282514]

Lock C, Hermans G, Pedotti R, Brendolan A, Schadt E, Garren H, Langer-Gould A, Strober S, Cannella B, Allard J, Klonowski P, Austin A, Lad N, Kaminski N, Galli SJ, Oksenberg JR, Raine CS, Heller R, Steinman L. Gene-microarray analysis of multiple sclerosis lesions yields new targets validated in autoimmune encephalomyelitis. Nat Med. 2002; 8:500–508. [PubMed: 11984595]

Lubberts E. IL-17/Th17 targeting: on the road to prevent chronic destructive arthritis? Cytokine. 2008; 41:84–91. [PubMed: 18039580]

Lubberts E, Schwarzenberger P, Huang W, Schurr JR, Peschon JJ, van den Berg WB, Kolls JK. Requirement of IL-17 receptor signaling in radiation-resistant cells in the joint for full progression of destructive synovitis. J Immunol. 2005; 175:3360–3368. [PubMed: 16116229]

Luchtman DW, Ellwardt E, Larochelle C, Zipp F. IL-17 and related cytokines involved in the pathology and immunotherapy of multiple sclerosis: Current and future developments. Cytokine Growth Factor Rev. 2014; 25:403–413. [PubMed: 25153998]

Mardiguian S, Serres S, Ladds E, Campbell SJ, Wilainam P, McFadyen C, McAteer M, Choudhury RP, Smith P, Saunders F, Watt G, Sibson NR, Anthony DC. Anti-IL-17A treatment reduces clinical score and VCAM-1 expression detected by in vivo magnetic resonance imaging in chronic relapsing EAE ABH mice. Am J Pathol. 2013; 182:2071–2081. [PubMed: 23602647]

Marwaha AK, Leung NJ, McMurchy AN, Levings MK. TH17 Cells in autoimmunity and immunodeficiency: protective or pathogenic? Front Immunol. 2012; 3:129. [PubMed: 22675324]

Matusevicius D, Kivisakk P, He B, Kostulas N, Ozenci V, Fredrikson S, Link H. Interleukin-17 mRNA expression in blood and CSF mononuclear cells is augmented in multiple sclerosis. Mult Scler. 1999; 5:101–104. [PubMed: 10335518]

McFarland HF, Martin R. Multiple sclerosis: a complicated picture of autoimmunity. Nat Immunol. 2007; 8:913–919. [PubMed: 17712344]

Mease PJ, Genovese MC, Greenwald MW, Ritchlin CT, Beaulieu AD, Deodhar A, Newmark R, Feng J, Erondu N, Nirula A. Brodalumab, an anti-IL17RA monoclonal antibody, in psoriatic arthritis. N Engl J Med. 2014; 370:2295–2306. [PubMed: 24918373]

Michalski D, Liebig S, Thomae E, Singer S, Hinz A, Bergh FT. Anxiety, depression and impaired health-related quality of life are therapeutic challenges in patients with multiple sclerosis. Ment Illn. 2010; 2:e5. [PubMed: 25478088]

Miller DH, Leary SM. Primary-progressive multiple sclerosis. Lancet Neurol. 2007; 6:903–912. [PubMed: 17884680]

Miller SD, Karpus WJ, Davidson TS. Experimental autoimmune encephalomyelitis in the mouse. Chapter 15, Unit. Curr Protoc Immunol. 2010

Milo R, Miller A. Revised diagnostic criteria of multiple sclerosis. Autoimmun Rev. 2014; 13:518–524. [PubMed: 24424194]

Moore S, Khalaj AJ, Patel R, Yoon J, Ichwan D, Hayardeny L, Tiwari-Woodruff SK. Restoration of axon conduction and motor deficits by therapeutic treatment with glatiramer acetate. J Neurosci Res. 2014; 92:1621–1636. [PubMed: 24989965]

Murugaiyan G, da Cunha AP, Ajay AK, Joller N, Garo LP, Kumaradevan S, Yosef N, Vaidya VS, Weiner HL. MicroRNA-21 promotes Th17 differentiation and mediates experimental autoimmune encephalomyelitis. J Clin Invest. 2015; 125:1069–1080. [PubMed: 25642768]

Nascimento MS, Carregaro V, Lima-Junior DS, Costa DL, Ryffel B, Duthie MS, de JA, de Almeida RP, da Silva JS. Interleukin 17A acts synergistically with interferon gamma to promote protection against Leishmania infantum infection. J Infect Dis. 2015; 211:1015–1026. [PubMed: 25274569]

Niimi N, Kohyama K, Matsumoto Y. Therapeutic gene silencing with siRNA for IL-23 but not for IL-17 suppresses the development of experimental autoimmune encephalomyelitis in rats. J Neuroimmunol. 2013; 254:39–45. [PubMed: 22989513]

Nishikawa K, Seo N, Torii M, Ma N, Muraoka D, Tawara I, Masuya M, Tanaka K, Takei Y, Shiku H, Katayama N, Kato T. Interleukin-17 induces an atypical M2-like macrophage subpopulation that regulates intestinal inflammation. PLoS ONE. 2014; 9:e108494. [PubMed: 25254662]

Nurieva R, Yang XO, Martinez G, Zhang Y, Panopoulos AD, Ma L, Schluns K, Tian Q, Watowich SS, Jetten AM, Dong C. Essential autocrine regulation by IL-21 in the generation of inflammatory T cells. Nature. 2007; 448:480–483. [PubMed: 17581589]

O'Connor W Jr, Kamanaka M, Booth CJ, Town T, Nakae S, Iwakura Y, Kolls JK, Flavell RA. A protective function for interleukin 17A in T cell-mediated intestinal inflammation. Nat Immunol. 2009; 10:603–609. [PubMed: 19448631]

Oliveira SR, Simao AN, Kallaur AP, de Almeida ER, Morimoto HK, Lopes J, Dichi I, Kaimen-Maciel DR, Reiche EM. Disability in patients with multiple sclerosis: influence of insulin resistance, adiposity, and oxidative stress. Nutrition. 2014; 30:268–273. [PubMed: 24484677]

Penesova A, Vlcek M, Imrich R, Vernerova L, Marko A, Meskova M, Grunnerova L, Turcani P, Jezova D, Kollar B. Hyperinsulinemia in newly diagnosed patients with multiple sclerosis. Metab Brain Dis. 2015; 30:895–901. [PubMed: 25809135]

Planat-Benard V, Silvestre JS, Cousin B, Andre M, Nibbelink M, Tamarat R, Clergue M, Manneville C, Saillan-Barreau C, Duriez M, Tedgui A, Levy B, Penicaud L, Casteilla L. Plasticity of human adipose lineage cells toward endothelial cells: physiological and therapeutic perspectives. Circulation. 2004; 109:656–663. [PubMed: 14734516]

Platten M, Youssef S, Hur EM, Ho PP, Han MH, Lanz TV, Phillips LK, Goldstein MJ, Bhat R, Raine CS, Sobel RA, Steinman L. Blocking angiotensin-converting enzyme induces potent regulatory T cells and modulates TH1- and TH17-mediated autoimmunity. Proc Natl Acad Sci U S A. 2009; 106:14948–14953. [PubMed: 19706421]

Qian Y, Liu C, Hartupee J, Altuntas CZ, Gulen MF, Jane-Wit D, Xiao J, Lu Y, Giltiay N, Liu J, Kordula T, Zhang QW, Vallance B, Swaidani S, Aronica M, Tuohy VK, Hamilton T, Li X. The adaptor Act1 is required for interleukin 17-dependent signaling associated with autoimmune and inflammatory disease. Nat Immunol. 2007; 8:247–256. [PubMed: 17277779]

Qu N, Xu M, Mizoguchi I, Furusawa J, Kaneko K, Watanabe K, Mizuguchi J, Itoh M, Kawakami Y, Yoshimoto T. Pivotal roles of T-helper 17-related cytokines, IL-17, IL-22, and IL-23, in inflammatory diseases. Clin Dev Immunol. 2013; 2013:968549. [PubMed: 23956763]

Ragozzino ME, Unick KE, Gold PE. Hippocampal acetylcholine release during memory testing in rats: augmentation by glucose. Proc Natl Acad Sci U S A. 1996; 93:4693–4698. [PubMed: 8643466]

Rocca MA, Amato MP, De SN, Enzinger C, Geurts JJ, Penner IK, Rovira A, Sumowski JF, Valsasina P, Filippi M. Clinical and imaging assessment of cognitive dysfunction in multiple sclerosis. Lancet Neurol. 2015; 14:302–317. [PubMed: 25662900]

Rouvier E, Luciani MF, Mattei MG, Denizot F, Golstein P. CTLA-8, cloned from an activated T cell, bearing AU-rich messenger RNA instability sequences, and homologous to a herpesvirus saimiri gene. J Immunol. 1993; 150:5445–5456. [PubMed: 8390535]

Ruddy MJ, Wong GC, Liu XK, Yamamoto H, Kasayama S, Kirkwood KL, Gaffen SL. Functional cooperation between interleukin-17 and tumor necrosis factor-alpha is mediated by CCAAT/enhancer-binding protein family members. J Biol Chem. 2004; 279:2559–2567. [PubMed: 14600152]

Schwandner R, Yamaguchi K, Cao Z. Requirement of tumor necrosis factor receptor-associated factor (TRAF)6 in interleukin 17 signal transduction. J Exp Med. 2000; 191:1233–1240. [PubMed: 10748240]

Serra-de-Oliveira N, Boilesen SN, Prado de Franca CC, LeSueur-Maluf L, Zollner RL, Spadari RC, Medalha CC, Monteiro de CG. Behavioural changes observed in demyelination model shares similarities with white matter abnormalities in humans. Behav Brain Res. 2015; 287:265–275. [PubMed: 25843560]

Straus DS. TNFalpha and IL-17 cooperatively stimulate glucose metabolism and growth factor production in human colorectal cancer cells. Mol Cancer. 2013; 12:78. [PubMed: 23866118]

Sumowski JF, Leavitt VM. Cognitive reserve in multiple sclerosis. Mult Scler. 2013; 19:1122–1127. [PubMed: 23897894]

Taniguchi CM, Emanuelli B, Kahn CR. Critical nodes in signalling pathways: insights into insulin action. Nat Rev Mol Cell Biol. 2006; 7:85–96. [PubMed: 16493415]

Theaudin M, Romero K, Feinstein A. In multiple sclerosis anxiety, not depression, is related to gender. Mult Scler. 2015

Trebst C, Sorensen TL, Kivisakk P, Cathcart MK, Hesselgesser J, Horuk R, Sellebjerg F, Lassmann H, Ransohoff RM. CCR1+/CCR5+ mononuclear phagocytes accumulate in the central nervous system of patients with multiple sclerosis. Am J Pathol. 2001; 159:1701–1710. [PubMed: 11696431]

Tzartos JS, Friese MA, Craner MJ, Palace J, Newcombe J, Esiri MM, Fugger L. Interleukin-17 production in central nervous system-infiltrating T cells and glial cells is associated with active disease in multiple sclerosis. Am J Pathol. 2008; 172:146–155. [PubMed: 18156204]

Ulrich R, Kalkuhl A, Deschl U, Baumgartner W. Machine learning approach identifies new pathways associated with demyelination in a viral model of multiple sclerosis. J Cell Mol Med. 2010; 14:434–448. [PubMed: 19183246]

Waisman A, Hauptmann J, Regen T. The role of IL-17 in CNS diseases. Acta Neuropathol. 2015; 129:625–637. [PubMed: 25716179]

Wang C, Dehghani B, Li Y, Kaler LJ, Vandenbark AA, Offner H. Oestrogen modulates experimental autoimmune encephalomyelitis and interleukin-17 production via programmed death 1. Immunology. 2009; 126:329–335. [PubMed: 19302141]

Wang H, Li C, Wang H, Mei F, Liu Z, Shen HY, Xiao L. Cuprizone-induced demyelination in mice: age-related vulnerability and exploratory behavior deficit. Neurosci Bull. 2013; 29:251–259. [PubMed: 23558591]

Wens I, Dalgas U, Deckx N, Cools N, Eijnde B. Does multiple sclerosis affect glucose tolerance? Mult Scler. 2013; 20:1273–1276. [PubMed: 24347183]

Winer S, Chan Y, Paltser G, Truong D, Tsui H, Bahrami J, Dorfman R, Wang Y, Zielenski J, Mastronardi F, Maezawa Y, Drucker DJ, Engleman E, Winer D, Dosch HM. Normalization of obesity-associated insulin resistance through immunotherapy. Nat Med. 2009; 15:921–929. [PubMed: 19633657]

Yang J, Sundrud MS, Skepner J, Yamagata T. Targeting Th17 cells in autoimmune diseases. Trends Pharmacol Sci. 2014; 35:493–500. [PubMed: 25131183]

Zager A, Peron JP, Mennecier G, Rodrigues SC, Aloia TP, Palermo-Neto J. Maternal immune activation in late gestation increases neuroinflammation and aggravates experimental autoimmune encephalomyelitis in the offspring. Brain Behav Immun. 2015; 43:159–171. [PubMed: 25108214]

Zenobia C, Hajishengallis G. Basic biology and role of interleukin-17 in immunity and inflammation. Periodontol 2000. 2015; 69:142–159. [PubMed: 26252407]

Zepp J, Wu L, Li X. IL-17 receptor signaling and T helper 17-mediated autoimmune demyelinating disease. Trends Immunol. 2011; 32:232–239. [PubMed: 21493143]

Zhang X, Angkasekwinai P, Dong C, Tang H. Structure and function of interleukin-17 family cytokines. Protein Cell. 2011; 2:26–40. [PubMed: 21337007]

Zorzella-Pezavento SF, Chiuso-Minicucci F, Franca TG, Ishikawa LL, da Rosa LC, Marques C, Ikoma MR, Sartori A. Persistent inflammation in the CNS during chronic EAE despite local absence of IL-17 production. Mediators Inflamm. 2013; 2013:519627. [PubMed: 23970813]

Zuniga LA, Shen WJ, Joyce-Shaikh B, Pyatnova EA, Richards AG, Thom C, Andrade SM, Cua DJ, Kraemer FB, Butcher EC. IL-17 regulates adipogenesis, glucose homeostasis, and obesity. J Immunol. 2010; 185:6947–6959. [PubMed: 21037091]

Highlights

- IL-17A overexpression in the CNS does not cause physical and learning disabilities
- IL-17A overexpression improves glucose tolerance and insulin sensitivity
- IL-17A overexpression reduces epididymal adipose tissue mass
- IL-17A increases glucose uptake by AKT activation in PC12 cell

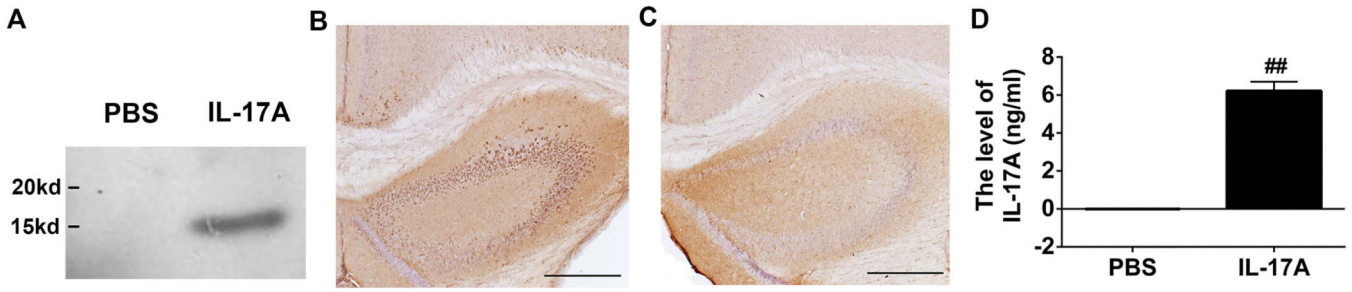

Figure 1. Overexpression of IL-17A in mouse brain

(A) Three months after rAAV5-IL-17A intraventricular injection, IL-17A was identified as an approximate 16 kDa fragment in the brain homogenate by western blot using anti-Flag M2 antibody. (B and C) Five months after the injection, IL-17A expression was found throughout the hippocampi and partly in neocortexes along the ventricles and hippocampi in IL-17A-in-Brain mice (B) while no positive staining was found in PBS-in-Brain mice (C). Scale bars are 500μm. (D) Nine months after injection, the levels of IL-17A in the plasma from IL-17A-in-Brain and PBS-in-Brain mice were determined by ELISA. ## P< 0.001.

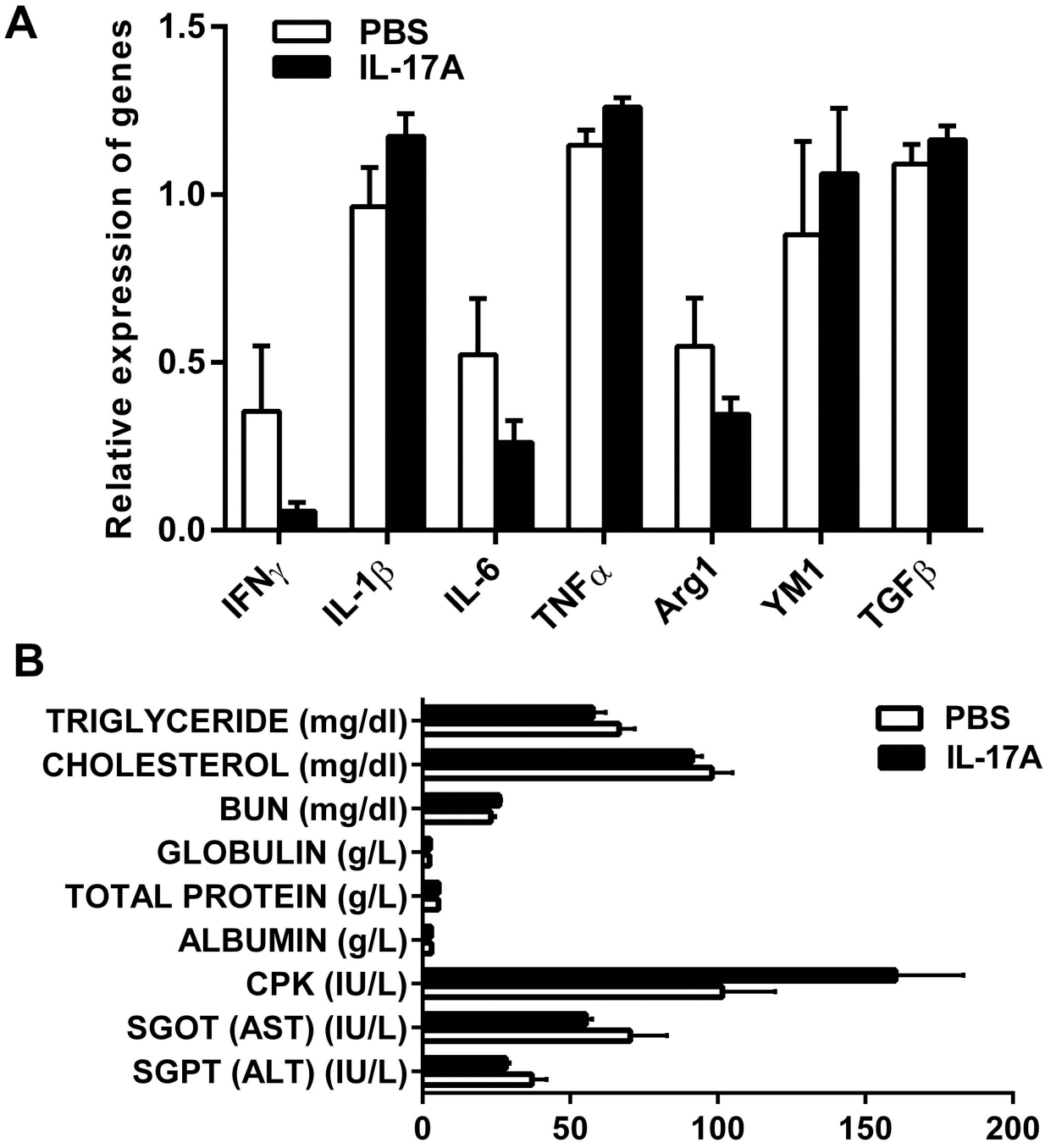

Figure 2. M1 and M2 macrophage/microglia markers and blood chemistry tests

(A) mRNA expression levels of M1 and M2 macrophage/microglia markers in the brains of IL-17A-in-Brain and PBS-in-Brain mice determined by real-time PCR are shown. The values were normalized to β-actin. No difference was found between the two groups (n=4 for each group). (B) Blood biochemical profiles in IL-17A-in-Brain and PBS-in-Brain mice. All values of the blood chemistry results and plasma creatinine levels (<0.2 mg/dl, not shown) are within normal ranges and show no differences between the two groups (n=4 for each group).

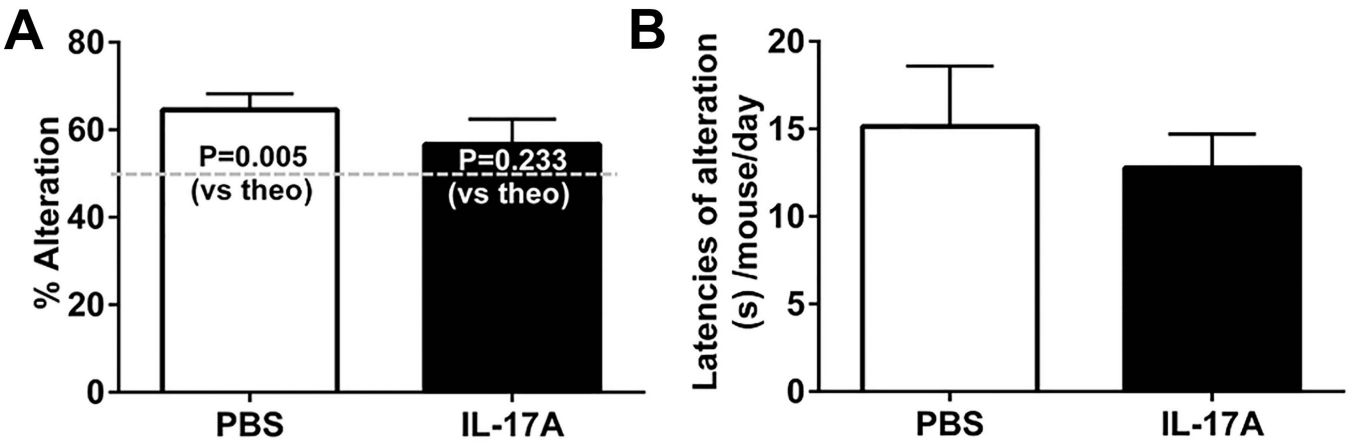

Figure 3. Effects of IL-17A overexpression on mice in T-maze

The number of alterations (A) and the latencies (B) before responding with 1 min cut-off are shown as means ± SEM. n = 8–10 for each group.

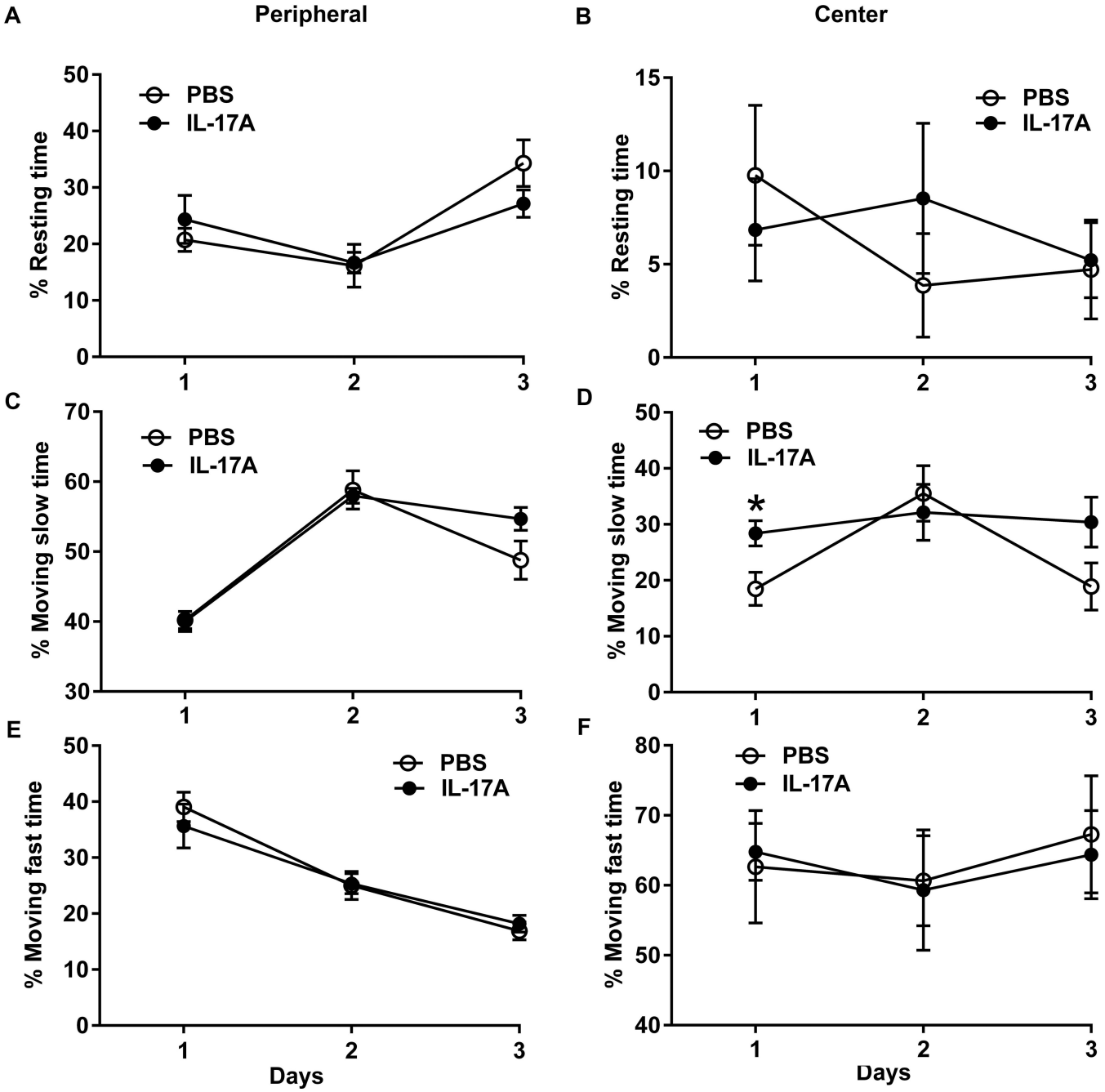

Figure 4. Effects of IL-17A overexpression on mice in open-field

The percentages of resting time in peripheral (A) and central (B) zones, of moving slow in peripheral (C) and central (D) zones, or moving fast in peripheral (E) and central (F) zones in a 5-min session are shown as means ± SEM for 3 days.

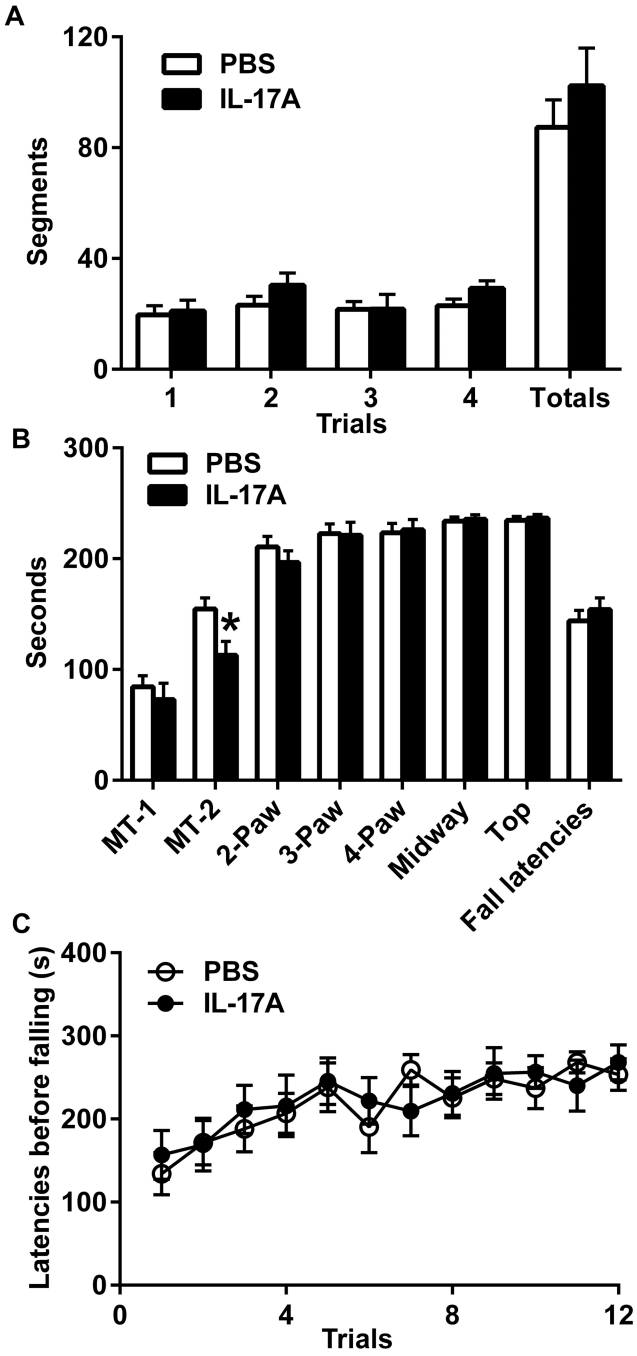

Figure 5. Effects of IL-17A overexpression on motor coordination

(A) The number of segments crossed before falling (means ± SEM) from stationary beam in 4-trial sessions. (B) The latencies before reaching MT-1, MT-2, 2 paws, 3 paws, 4 paws, midway point and top with 1-min cut-off. (C) The latencies before falling (means ± SEM) from the accelerating rotorod in 4-trial sessions for 3 days. * P<0.05.

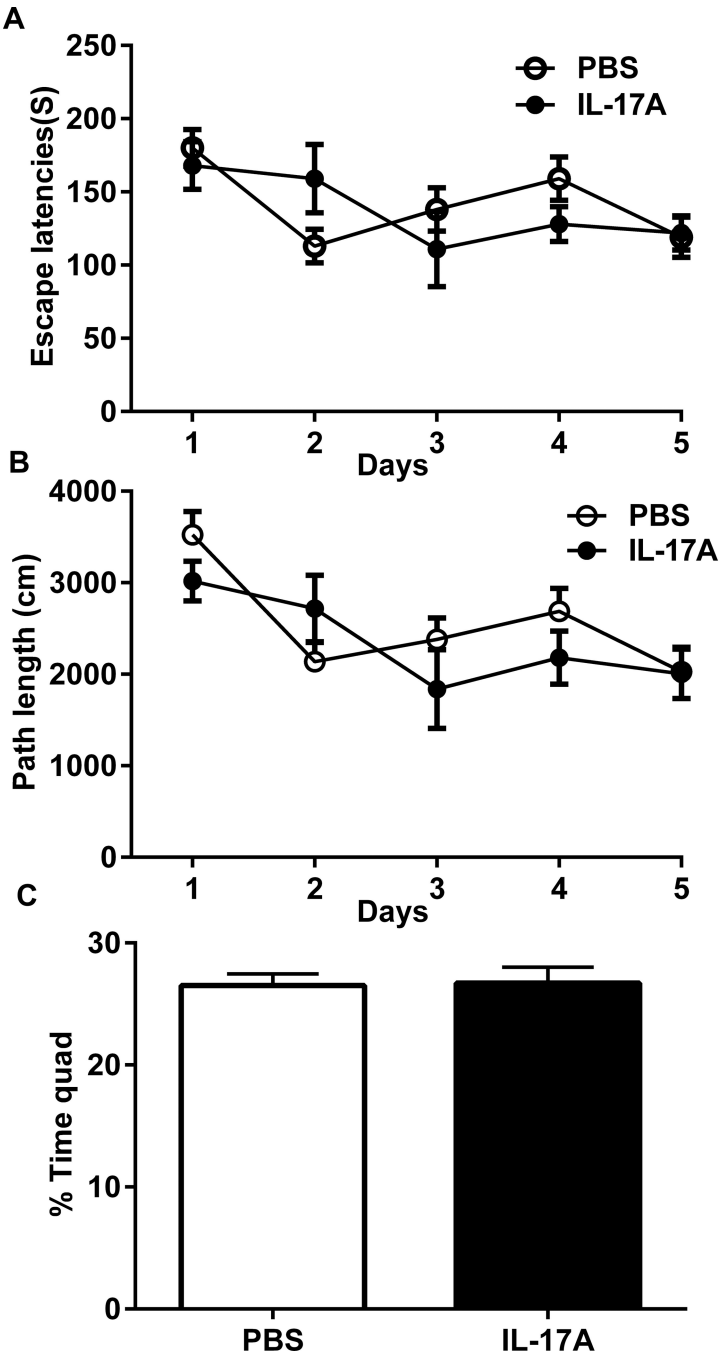

Figure 6. Effects of IL-17A overexpression on cognitive function in water maze

(A) Total escape latencies (s) and (B) total path lengths (cm) per day are shown as means ± SEM. (C) The probe trial of the Morris water maze. Percentages of time spent in the target quadrant in which the hidden platform was previously placed are shown.

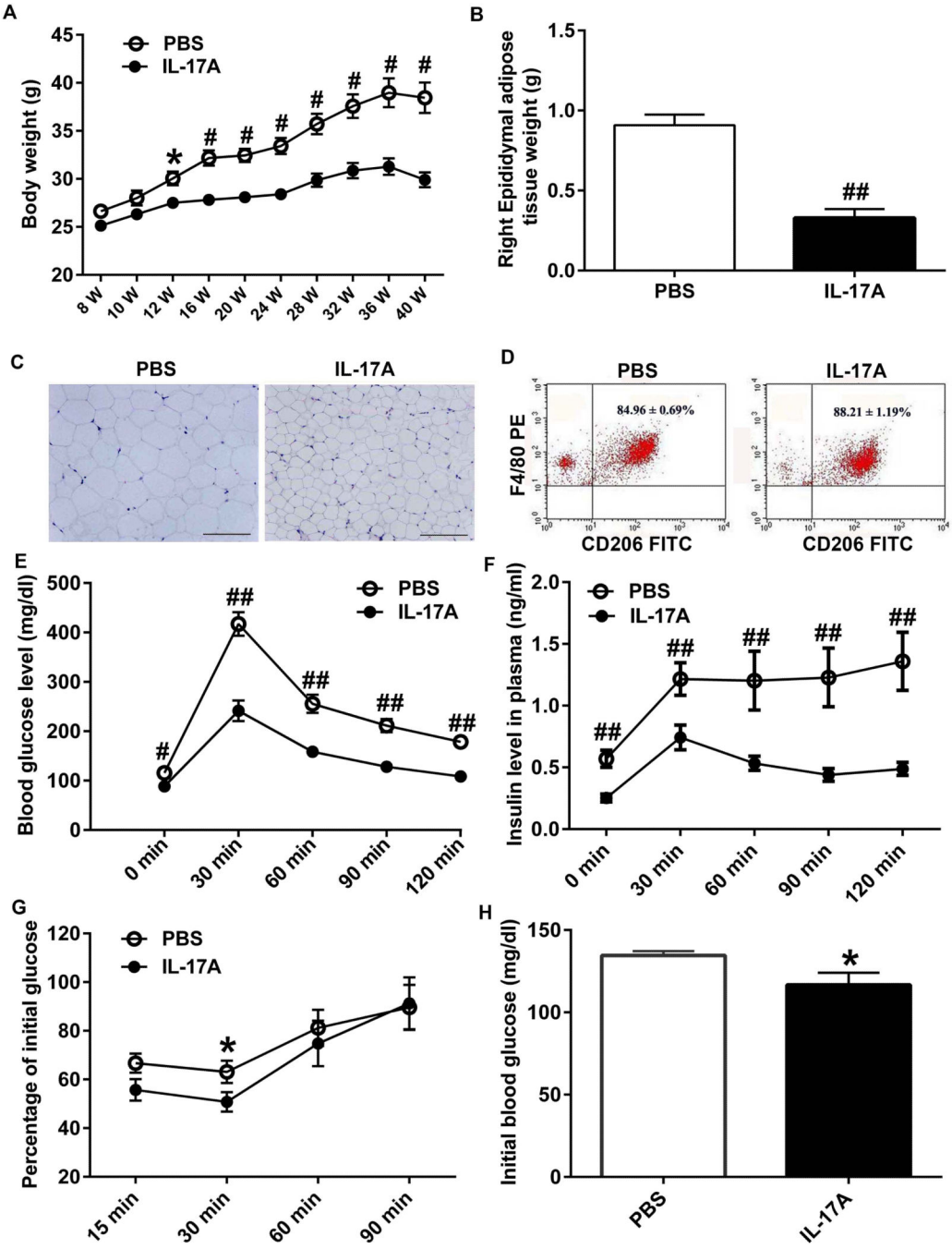

Figure 7. Effect of IL-17A overexpression on bodyweight, IPGTT, ITT and adipose tissue

(A) Two-month-old mice (n=9–11/each group) were subjected to intraventricular injection of PBS or rAAV5-IL-17A and their bodyweights were measured every two weeks. (B) Thirty-two weeks after the injection, mice were euthanized and epididymal adipose tissues were isolated. The average weight of right epididymal adipose tissues in IL-17A-in-Brain mice are approximately one third of that in PBS-in-Brain mice. (C) Haematoxylin and eosin-stained images of paraffin embedded epididymal adipose tissue sections from PBS-in-Brain and IL-17A-in-Brain mice. Scale bars are 200μm. (D) Flow cytometer analyses showing

expression levels of $CD206^+$ and $F4/80^+$ M2 macrophages in the adipose tissues. (E and F) Twenty weeks after injection, mice were fasted for 16 h and injected i.p. with 1.5 g glucose/kg bodyweight and blood glucose and insulin were measured before and after glucose injection at the indicated time points. (G) Thirty weeks after PBS or rAAV5-IL-17A injection, mice were fasted for 6 h and injected i.p. with 0.75 U insulin/kg bodyweight for ITT. Blood glucose levels were determined and are shown as percent changes from (H) basal blood glucose levels. * $P < 0.05$, # $P < 0.01$ and ## $P < 0.001$.

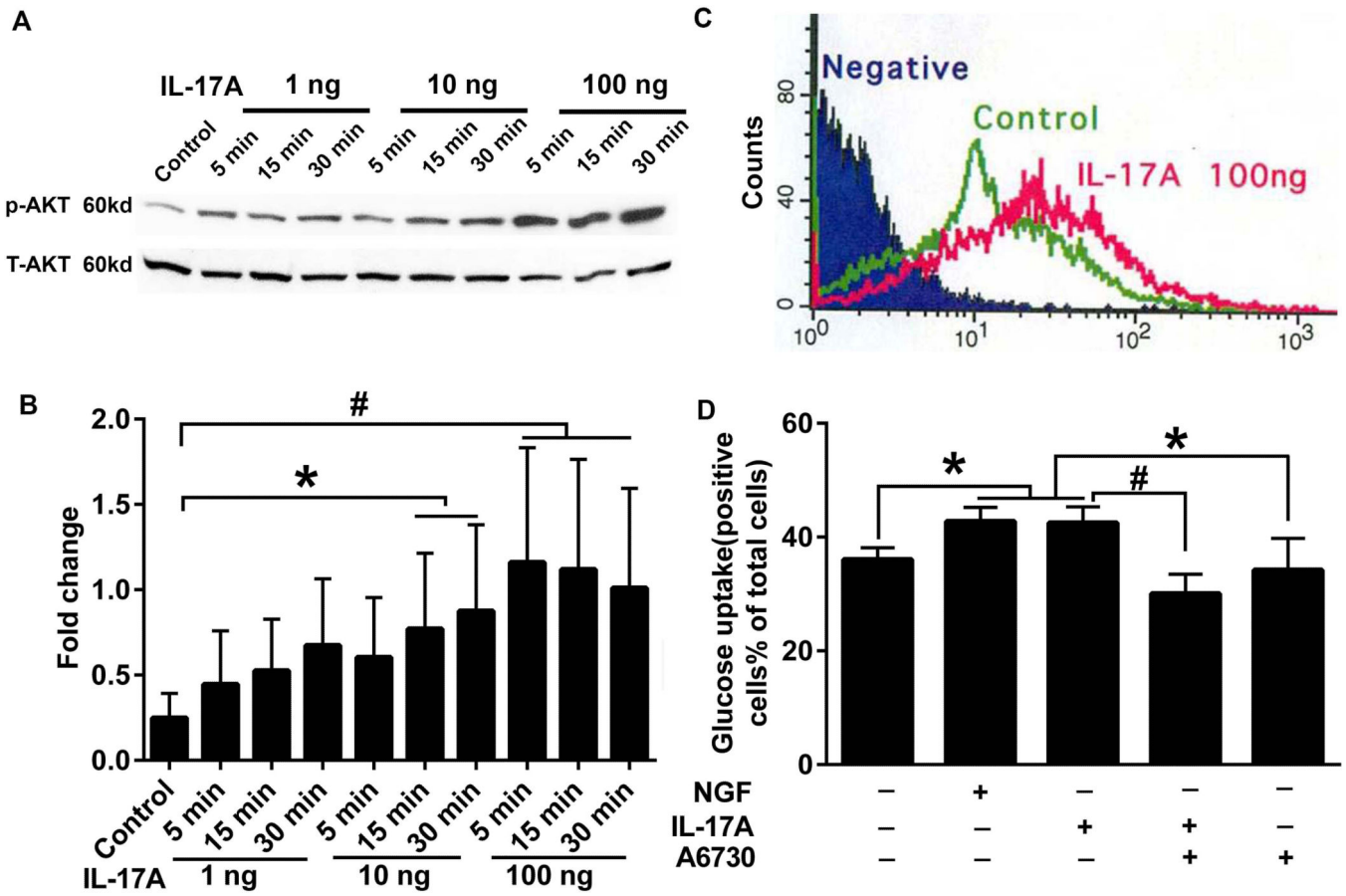

Figure 8. Effect of IL-17A on activation of Akt and glucose uptake

(A) PC12 cells were treated with 1, 10 and 100 ng/ml IL-17A for 5, 15 and 30 min. The cell lysates were analyzed by western blotting using phospho-Akt (S473, p-Akt) and total-Akt (T-Akt) antibodies. (B) The bar graph represents the results of densitometric analysis of western blots shown in A. (C) PC12 cells were treated with or without IL-17A 100 ng/ml for 30 min followed by treatment with 2-NBDG for 10 min. Glucose uptake curves by flow cytometer are shown. Negative and Control stand for PC12 cells prepared without 2-NBDG and IL-17A treatment, respectively. Glucose uptake curve of PC12 cells treated with NGF is identical to that of IL-17A-treated PC12 cells (not shown). (D) PC12 cells were pretreated with or without Akt 1/2 inhibitor, A6730, for 30 min followed by treatment with or without 100 ng/ml IL-17A. NGF (100 ng/ml) treatment serves as a positive control. Bar graphs present percentages of PC12 cells that show glucose uptake by flow cytometer (D). The statistical results, * $P<0.05$ and # $P<0.01$, are from three independent experiments as shown in B and D.

Table 1

Real-time PCR primer sequence

	Forword (5'-3')	**Reverse (5'-3')**
IFNγ	TCAAGTGGCATAGATGTGGAAGAA	TGGCTCTGCAGGATTTTCATG
IL-1β	GCAACTGTTCCTGAACTCAACT	ATCTTTTGGGGTCCGTCAACT
IL-6	TAGTCCTTCCTACCCCAATTTCC	TTGGTCCTTAGCCACTCCTTC
TNFα	CCCTCACACTCAGATCATCTTCT	GCTACGACGTGGGCTACAG
Arg1	CACTCCCCTGACAACCAGCT	AAGGACACAGGTTGCCCATG
YM1	CAGGTCTGGCAATTCTTCTGAA	GTCTTGCTCATGTGTGTAAGTGA
TGFβ	CTCCCGTGGCTTCTAGTGC	GCCTTAGTTTGGACAGGATCTG
β-actin	GGCTGTATTCCCCTCCATCG	CCA GTTGGTAACAATGCCATGT

Table 2

Effects of IL-17A on exploratory activity in plus-maze (means ± SEM)

Measures	PBS	IL-17A
Day 1		
Open arms		
Entries	13.5 ± 1.2	13 ± 1.4
Duration (s)	74.4 ± 10.5	82.0 ± 10.0
Enclosed arms		
Entries	14.4 ± 0.8	12.3 ± 1.0
Duration (s)	162.3 ± 13.8	181.2 ± 9.7
Open/total ratio (%)		
Entries	47.8 ± 2.2	50.9 ± 2.7
Duration	26.5 ± 3.1	27.3 ± 3.3
Day 2		
Open arms		
Entries	6.6 ± 1.2	6.9 ± 1.0
Duration (s)	42.4 ± 7.8	32.4 ± 6.7
Enclosed arms		
Entries	11.0 ± 0.9	10.7 ± 1.3
Duration (s)	227.1 ± 10.1	242.1 ± 9.7
Open/total ratio (%)		
Entries	35.4 ± 3.3	39.1 ± 1.6
Duration	14.1 ± 2.6	10.8 ± 2.2